

HIGH PRECISION LEPTON PAIR BREMSSTRAHLUNG WITH PHOTOS*

S. ANTROPOV

H. Niewodniczański Institute of Nuclear Physics Polish Academy of Sciences
31-342 Kraków, Poland

(Received May 7, 2020)

I present results for the final-state emissions of lepton pairs in decays of heavy intermediate states such as Z boson. Numerical distributions of relevance for the LHC are shown. A testing framework allowing comparison of spectra by PHOTOS with an exact one solution is developed. Exact matrix element of $2f \rightarrow Z/\gamma^* \rightarrow 4f$ process has been installed into PHOTOS and has been tested. Approximation of exact matrix element is proposed and future research is suggested in order to factorize approximated matrix element.

DOI:10.5506/APhysPolB.51.1221

1. Introduction

One of the purposes of the LHC experiments is to improve precision of the W -boson mass measurement. Precision measurements of the W -boson mass rely on a precise reconstruction of momenta for the final-state leptons [1] and on comparison of W -boson production and decay with those of Z boson. The QED effects of the final-state radiation play an important role in such experimental studies [2]. Final-state bremsstrahlung is included in all simulation chains and should be studied together with the detector response to leptons.

Precise calculations of interesting quantities must include such radiative corrections of precision level of the order of $\sim 0.1\%$, they are usually calculated with a help of MC generators in order to take into account detector acceptance simultaneously. The experimental data are compared to expectations from MC simulation. In the study [1], it is specifically stated that “the dominant source of electroweak corrections to W - and Z -boson production

* Presented at XXVI Cracow Epiphany Conference on LHC Physics: Standard Model and Beyond, Kraków, Poland, January 7–10, 2020.

originates from QED final-state radiation, and is simulated with PHOTOS” and that “Final-state lepton pair production, through $\gamma^* \rightarrow$ lepton pair, constitutes a significant additional source of energy loss for the W -boson decay products”. The present paper is focused on improvement of PHOTOS [3–9] algorithm for simulation of the additional lepton pair emissions in decays of γ^* and Z boson, see Fig. 2.

The paper is organized as follows: Section 2 contains description of matrix element to be tested in PHOTOS; Section 3 collects results of the tests; brief Summary is at the end.

2. Pair emission matrix element

By M_{Born} I depict matrix element of Fig. 1, by M_1, M_2, M_3, M_4 I depict matrix elements of Fig. 2. In the following, I define four momenta as they are presented on the Feynman diagrams of Figs. 1–2.

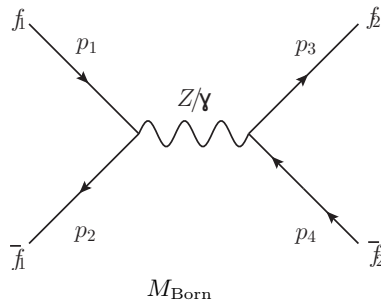


Fig. 1. The Feynman diagram corresponding to $f_1(p_1)\bar{f}_1(p_2) \rightarrow Z/\gamma^* \rightarrow f_2(p_3)\bar{f}_2(p_4)$ Born level process.

PHOTOS feature extra pair emission for any $Z/\gamma^* \rightarrow ll$ decay is based on soft factorized matrix element (see Ref. [10]), which is the soft limit of the complete pair emission matrix element $\sum_{\text{spins}} |M_1 + M_2|^2$ of the form which can be used all over the phase space

$$\sum_{\text{spins}} |M_1 + M_2|_{\text{soft}}^2 = F_{\text{soft}}(p_1, p_2; p_3, p_4, p_5, p_6) \cdot |M(p_1, p_2; p'_3, p'_4)|_{\text{Born}}^2, \quad (1)$$

where $p_1, p_2, p_3, p_4, p_5, p_6, q$ are four momenta that are described by Fig. 2; p'_3, p'_4 are four momenta of two-body phase space (*i.e.* $p_1^\mu + p_2^\mu = (p'_3)^\mu + (p'_4)^\mu$);

$$|M|_{\text{Born}}^2 = \frac{\alpha^2 (4\pi)^2}{(p_1 + p_2)^4} \text{Tr}[(\not{p}_1 + m_1) \gamma_\mu (\not{p}_2 - m_1) \gamma_\nu] \times \text{Tr}[(\not{p}'_3 + m_2) \gamma^\mu (\not{p}'_4 - m_2) \gamma^\nu] \quad (2)$$

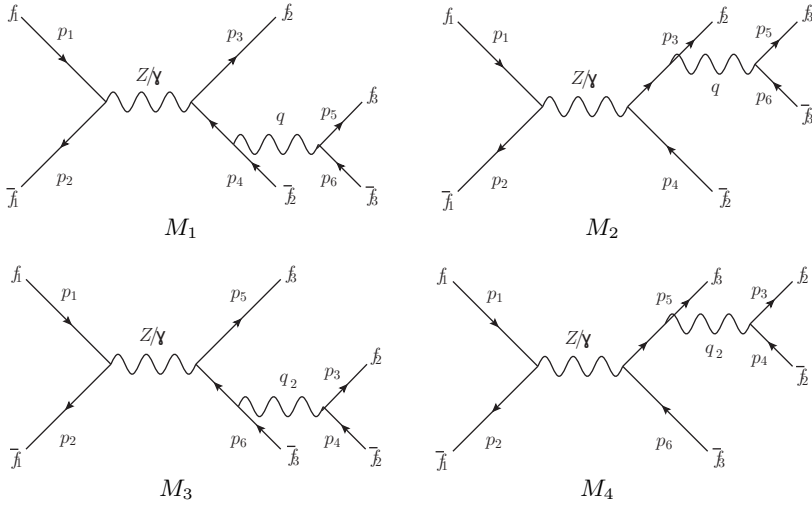


Fig. 2. Feynman diagrams corresponding to $f_1(p_1)\bar{f}_1(p_2) \rightarrow Z/\gamma^* \rightarrow f_2(p_3)\bar{f}_2(p_4)f_3(p_5)\bar{f}_3(p_6)$ process.

is the Born level matrix element, α is QED constant and

$$F_{\text{soft}} = 2(4\pi\alpha)^2 \frac{4p_5^\alpha p_6^\beta - q^2 \cdot g^{\alpha\beta}}{q^4} \left(\frac{p_3^\alpha}{p_3 q} - \frac{p_4^\alpha}{p_4 q} \right) \left(\frac{p_3^\beta}{p_3 q} - \frac{p_4^\beta}{p_4 q} \right) \quad (3)$$

is factorized part of matrix element. This factorization property of QED is important for PHOTOS design, in particular for construction of its algorithm of pair emission. On its basis, a universal pair emission algorithm, which can provide reasonable results for any process, is established. The Born level process $|M|_{\text{Born}}^2$ is managed by other than PHOTOS MC generator. Then events of the Born level process are modified according to F_{soft} factorized part of matrix element.

I focus on analysis of matrix element $\sum_{\text{spins}} |M_1 + M_2|^2$ for an $2f \rightarrow Z/\gamma^* \rightarrow 4f$ spin summated process of Fig. 2 and on indication of its tensor components ($H_i^{\mu,\nu}$, $i = 1 \dots 8$) that are small giving small invariant mass of extra pair. Matrix element $\sum_{\text{spins}} |M_1 + M_2|^2$ reads

$$\sum_{\text{spins}} |M_1 + M_2|^2 = \sum_{\text{spins}} |M_1 + M_2|_{\text{soft}}^2 + \frac{\alpha^4 (4\pi)^4}{(p_1 + p_2)^4 q^4} \times \text{Tr}[(\not{p}_1 + m_1) \gamma_\mu (\not{p}_2 - m_1) \gamma_\nu] \times \sum_{i=1}^8 H_i^{\mu,\nu}, \quad (4)$$

where

$$H_1^{\mu,\nu} = \frac{16}{(2(p_3q) + q^2)(2(p_4q) + q^2)} \times \left[\text{Tr} [q_2 \gamma^\mu q \gamma^\nu] \left(p_3 p_4 \frac{q^2}{2} \right) - 4g^{\mu,\nu} \left(2m_3^2 \frac{q^2}{2} 2p_3 p_4 \right) \right], \quad (5)$$

$$H_2^{\mu,\nu} = \frac{16}{(2(p_3q) + q^2)^2} \left[\text{Tr} [\not{p}_4 \gamma^\mu (\not{p}_5 - \not{p}_6) \gamma^\nu] \frac{q^2}{2} \cdot p_3 (p_5 - p_6) \right] + \frac{16}{(2(p_4q) + q^2)^2} \left[\text{Tr} [\not{p}_3 \gamma^\mu (\not{p}_5 - \not{p}_6) \gamma^\nu] \frac{q^2}{2} \cdot p_4 (p_5 - p_6) \right], \quad (6)$$

$$H_3^{\mu,\nu} = \frac{16}{(2(p_3q) + q^2)^2} \left[\text{Tr} [\not{p}_3 \gamma^\mu \not{p}_4 \gamma^\nu] \frac{q^2}{2} \cdot p_3 q \right] - \frac{16}{(2(p_3q) + q^2)(2(p_4q) + q^2)} \left[\text{Tr} [\not{p}_3 \gamma^\mu \not{p}_3 \gamma^\nu] p_4 q \frac{q^2}{2} \right] + \frac{16}{(2(p_4q) + q^2)^2} \left[\text{Tr} [\not{p}_3 \gamma^\mu \not{p}_4 \gamma^\nu] \frac{q^2}{2} \cdot p_4 q \right] - \frac{16}{(2(p_3q) + q^2)(2(p_4q) + q^2)} \left[\text{Tr} [\not{p}_4 \gamma^\mu \not{p}_4 \gamma^\nu] p_3 q \frac{q^2}{2} \right], \quad (7)$$

$$H_4^{\mu,\nu} = \frac{16}{(2(p_3q) + q^2)^2} \left[-2\text{Tr} [\not{p}_4 \gamma^\mu \not{p}_5 \gamma^\nu] (p_3 p_6)^2 - 2\text{Tr} [\not{p}_4 \gamma^\mu \not{p}_6 \gamma^\nu] (p_3 p_5)^2 \right] + \frac{16}{(2(p_4q) + q^2)^2} \left[-2\text{Tr} [\not{p}_3 \gamma^\mu \not{p}_5 \gamma^\nu] (p_4 p_6)^2 - 2\text{Tr} [\not{p}_3 \gamma^\mu \not{p}_6 \gamma^\nu] (p_4 p_5)^2 \right] + \frac{16}{(2(p_3q) + q^2)(2(p_4q) + q^2)} \times [2\text{Tr} [\not{p}_3 \gamma^\mu \not{p}_6 \gamma^\nu] (p_3 p_5 \cdot p_4 p_5) + 2\text{Tr} [\not{p}_4 \gamma^\mu \not{p}_6 \gamma^\nu] (p_3 p_5 \cdot p_4 p_5) + 2\text{Tr} [\not{p}_3 \gamma^\mu \not{p}_5 \gamma^\nu] (p_3 p_6 \cdot p_4 p_6) + 2\text{Tr} [\not{p}_4 \gamma^\mu \not{p}_5 \gamma^\nu] (p_3 p_6 \cdot p_4 p_6)], \quad (8)$$

$$H_5^{\mu,\nu} = \frac{16}{(2(p_3q) + q^2)^2} \left[4g^{\mu,\nu} m_2^2 \frac{q^2}{2} \left(\frac{q^2}{2} + m_3^2 \right) - \text{Tr} [\not{p}_4 \gamma^\mu \not{p}_5 \gamma^\nu] m_2^2 \frac{q^2}{2} \right] - \text{Tr} [\not{p}_4 \gamma^\mu \not{p}_6 \gamma^\nu] m_2^2 \frac{q^2}{2} \left[+ \frac{16}{(2(p_4q) + q^2)^2} \left[4g^{\mu,\nu} m_2^2 \frac{q^2}{2} \left(\frac{q^2}{2} + m_3^2 \right) \right] \right] - \text{Tr} [\not{p}_3 \gamma^\mu \not{p}_5 \gamma^\nu] m_2^2 \frac{q^2}{2} - \text{Tr} [\not{p}_3 \gamma^\mu \not{p}_6 \gamma^\nu] m_2^2 \frac{q^2}{2} \left[\right]$$

$$\begin{aligned}
 & + \frac{16}{(2(p_3q) + q^2)(2(p_4q) + q^2)} \left[-2\text{Tr} [\not{p}_5\gamma^\mu\not{p}_6\gamma^\nu] (m_2^2m_3^2) \right. \\
 & - 4g^{\mu,\nu} \left(2m_3^2\frac{q^2}{2}m_2^2 \right) \\
 & \left. - (\text{Tr} [\not{p}_5\gamma^\mu\not{p}_5\gamma^\nu] + \text{Tr} [\not{p}_6\gamma^\mu\not{p}_6\gamma^\nu]) \left(m_2^2\frac{q^2}{2} + m_3^2m_2^2 \right) \right], \quad (9)
 \end{aligned}$$

$$\begin{aligned}
 H_6^{\mu,\nu} = & \frac{16}{(2(p_3q) + q^2)(2(p_4q) + q^2)} \\
 & \times [-2\text{Tr} [\not{p}_5\gamma^\mu\not{p}_6\gamma^\nu] (p_3p_6 \cdot p_4p_5 + p_3p_5 \cdot p_4p_6) \\
 & + 2\text{Tr} [\not{p}_6\gamma^\mu\not{p}_6\gamma^\nu] (p_3p_5 \cdot p_4p_5) + 2\text{Tr} [\not{p}_5\gamma^\mu\not{p}_5\gamma^\nu] (p_3p_6 \cdot p_4p_6) \\
 & + 4g^{\mu,\nu} (2m_3^2(p_3p_5 \cdot p_4p_5 + p_3p_6 \cdot p_4p_6) \\
 & \times - 2p_5p_6(p_3p_6 \cdot p_4p_5 + p_3p_5 \cdot p_4p_6))] , \quad (10)
 \end{aligned}$$

$$\begin{aligned}
 H_7^{\mu,\nu} = & \frac{16}{(2(p_3q) + q^2)(2(p_4q) + q^2)} [2\text{Tr} [\not{p}_5\gamma^\mu\not{p}_6\gamma^\nu] p_3p_4 \cdot p_5p_6 \\
 & - (\text{Tr} [\not{p}_5\gamma^\mu\not{p}_5\gamma^\nu] + \text{Tr} [\not{p}_6\gamma^\mu\not{p}_6\gamma^\nu]) m_3^2 \cdot p_3p_4] , \quad (11)
 \end{aligned}$$

$$\begin{aligned}
 H_8^{\mu,\nu} = & 16m_3^2 \left(\frac{1}{(2(p_3q) + q^2)} + \frac{1}{(2(p_4q) + q^2)} \right) \left(\frac{\text{Tr} [\not{p}_3\gamma^\mu\not{q}\gamma^\nu] p_4q}{2p_4q + q^2} \right. \\
 & \left. + \frac{\text{Tr} [\not{p}_4\gamma^\mu\not{q}\gamma^\nu] p_3q}{2p_3q + q^2} - \frac{\text{Tr} [\not{p}_3\gamma^\mu\not{p}_4\gamma^\nu] \frac{q^2}{2}}{2(p_3q) + q^2} - \frac{\text{Tr} [\not{p}_3\gamma^\mu\not{p}_4\gamma^\nu] \frac{q^2}{2}}{2(p_4q) + q^2} \right), \quad (12)
 \end{aligned}$$

and where $\sum_{\text{spins}} |M_1 + M_2|_{\text{soft}}^2$ is defined now by

$$\sum_{\text{spins}} |M_1 + M_2|_{\text{soft}}^2 = F_{\text{soft}}(p_1, p_2; p_3, p_4, p_5, p_6) \cdot |M(p_1, p_2, p_3, p_4)|_{\text{Born}}^2 \cdot (13)$$

It differs from (1) by replacing four momenta p'_3, p'_4 by p_3, p_4 ; factorized part of soft matrix element F_{soft} is defined by formula (3); Born level matrix element $|M(p_1, p_2; p_3, p_4)|_{\text{Born}}^2$ is defined by formula (2); four momenta $p_1, p_2, p_3, p_4, p_5, p_6, q, q_2$ and masses m_1, m_2, m_3 of particles are defined as in Fig. 2.

3. Numerical results

The best test of PHOTOS generated spectra for the process $ee \rightarrow Z \rightarrow 4l$ is given by KORALW–PHOTOS comparison [11–13]. For most of technical details of simulation, see Ref. [12]. This comparison [12, 13] provides source of benchmarks for testing of extra pair matrix elements. Both PHOTOS

and KORALW have well-separated segments for exact phase-space description and matrix element calculations, which is exact in KORALW but of approximation in PHOTOS.

KORALW [11] feature both complete and exact matrix element for Z production and decay to four fermions. While emission of extra pair from the initial state in KORALW is switched off, its matrix element corresponds to four Feynman graphs presented in Fig. 2. For switching off an extra pair emission from the initial state in KORALW, the center-of-mass energy is set to equal Z -boson mass, and Z width is set to a very small value. The KORALW Monte Carlo has been used to simulate $e^+e^- \rightarrow Z \rightarrow e^+e^-\mu^+\mu^-$ channel.

A way to generate complete $4f$ end-state spectra by PHOTOS is to apply its algorithm over two PYTHIA [14] runs, *i.e.* $f_1\bar{f}_1 \rightarrow Z/\gamma^* \rightarrow f_2\bar{f}_2$ and $f_1\bar{f}_1 \rightarrow Z/\gamma^* \rightarrow f_3\bar{f}_3$. During the first run, PHOTOS generates extra $f_3\bar{f}_3$ pair for a Born level process $f_1\bar{f}_1 \rightarrow Z/\gamma^* \rightarrow f_2\bar{f}_2$ (M_1 and M_2 from Fig. 2), during the second run, PHOTOS generates extra $f_2\bar{f}_2$ pair for a Born level process $f_1\bar{f}_1 \rightarrow Z/\gamma^* \rightarrow f_3\bar{f}_3$ (M_3 and M_4 from Fig. 2).

For the test, 10^6 events are generated in the $e^+e^-\mu^+\mu^-$ channel by KORALW. For each test of PHOTOS kernel 3.665×10^8 $e^+e^- \rightarrow Z \rightarrow e^+e^-$ events and 3.665×10^8 $e^+e^- \rightarrow Z \rightarrow \mu^+\mu^-$ events is generated by PYTHIA at the CMS energy of 91.187 GeV, with the narrow up and down limits on CMS energy (91.17 GeV and 91.2 GeV respectively); then 1.002×10^6 events are generated by PYTHIA-PHOTOS in the $e^+e^-\mu^+\mu^-$ channel.

PHOTOS generated spectra are compared in the $Z \rightarrow e^+e^-\mu^+\mu^-$ channel with the ones obtained from KORALW. Figure 3 presents spectra of squared mass of e^+e^- pair ($M_{e^+e^-}^2$) and of $\mu^+\mu^-$ pair ($M_{\mu^+\mu^-}^2$) and ratios of PHOTOS generated spectra to the corresponding ones by KORALW. These spectra are of the most interest, since pair masses $M_{e^+e^-}$ and $M_{\mu^+\mu^-}$ are experiment observables [1]. Agreement between KORALW generated spectra and basic PHOTOS [9] generated spectra is the best for the most populated bins of each spectrum, for the minima of spectra, the highest disagreement between basic PHOTOS [9] and KORALW is observed. This disagreement stands for lack in generation of e^+e^- and $\mu^+\mu^-$ extra pairs of the highest energy. On the other hand, agreement between PHOTOS with matrix element (4) and KORALW is good; the ratio between numbers of PHOTOS events and KORALW events for any bin never differs from 1 more than 22%. Such a difference is vanishing with statistics increase. This agreement is remarkable since the interference between diagrams M_1 , M_2 and M_3 , M_4 is ignored in matrix element (4). However, all of the generated by PHOTOS extra pairs are of small invariant mass, therefore, an effect of gauge invariance breakdown is negligible.

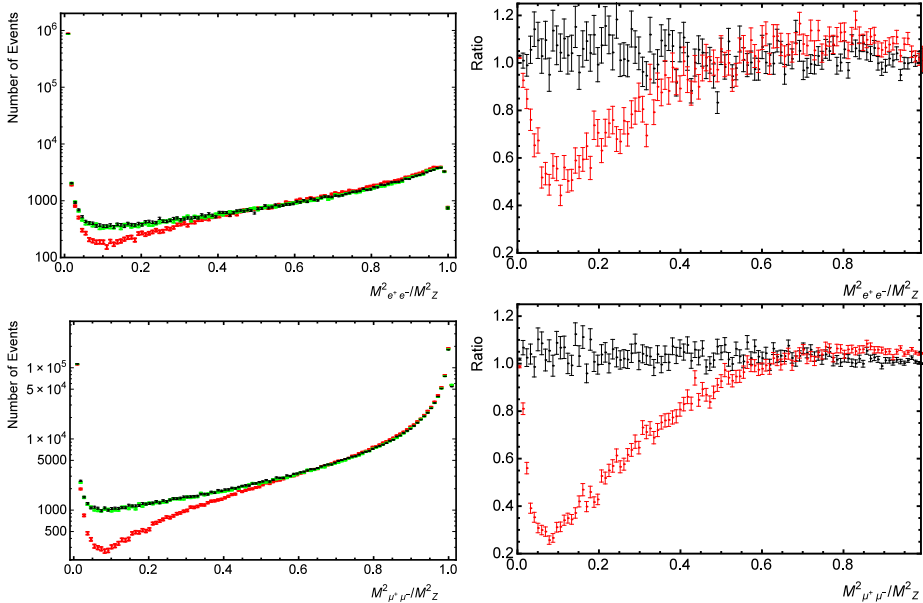


Fig. 3. (Colour on-line) Lepton pair invariant mass spectra in the channel $Z \rightarrow \mu^+ \mu^- e^+ e^-$. Top and bottom right: Ratios of PHOTOS generated spectra to the ones generated by KORALW. Dark grey (red) error bars represent data by PHOTOS with default matrix element (1). Black error bars represent data by PHOTOS with full matrix element (4). Top left: Spectra of electron pair mass squared. Bottom left: Spectra of muon pair mass squared. Light grey (green) error bars represent data by KORALW, where four fermion final-state matrix elements is used.

Having agreement between PHOTOS with matrix element (4) and KORALW verified, in order to approximate matrix element (4), I estimate an effect of each tensor $H_i^{\mu,\nu}$ on the extra pair emission. I perform simulations by PHOTOS with matrix element (4) missing one of the tensor $H_i^{\mu,\nu}$. For each test of PHOTOS kernel, 4.29×10^5 events are generated by PYTHIA-PHOTOS in the $e^+ e^- \mu^+ \mu^-$ channel and the results are presented in Fig. 4.

Figure 4 presents ratios of PHOTOS generated spectra of squared mass of $e^+ e^-$ pair ($M_{e^+ e^-}^2$) and of $\mu^+ \mu^-$ pair ($M_{\mu^+ \mu^-}^2$) to the corresponding one's by PHOTOS with matrix element (4) in the $e^+ e^- \mu^+ \mu^-$ channel. From Fig. 4 it is seen that tensors $H_1^{\mu,\nu} - H_4^{\mu,\nu}$ are of most importance for precision spectra generation, while tensors $H_5^{\mu,\nu} - H_8^{\mu,\nu}$ can be easily dropped off from the matrix element (4). In all the tests, the number of pairs with invariant mass close to M_Z ($M_{e^+ e^-}^2 \sim M_Z^2$, $M_{\mu^+ \mu^-}^2 \sim M_Z^2$) matches the one from the corresponding etalon spectra. The first bin of the $e^+ e^-$ pair spectrum contains vast majority of generated extra pairs, their number indicates general

performance of the pair emission algorithm. The number of pairs with the smallest invariant mass ($M_{e^+e^-}^2 \sim 0$, $M_{\mu^+\mu^-}^2 \sim 0$) rarely matches the one from the corresponding etalon spectra.

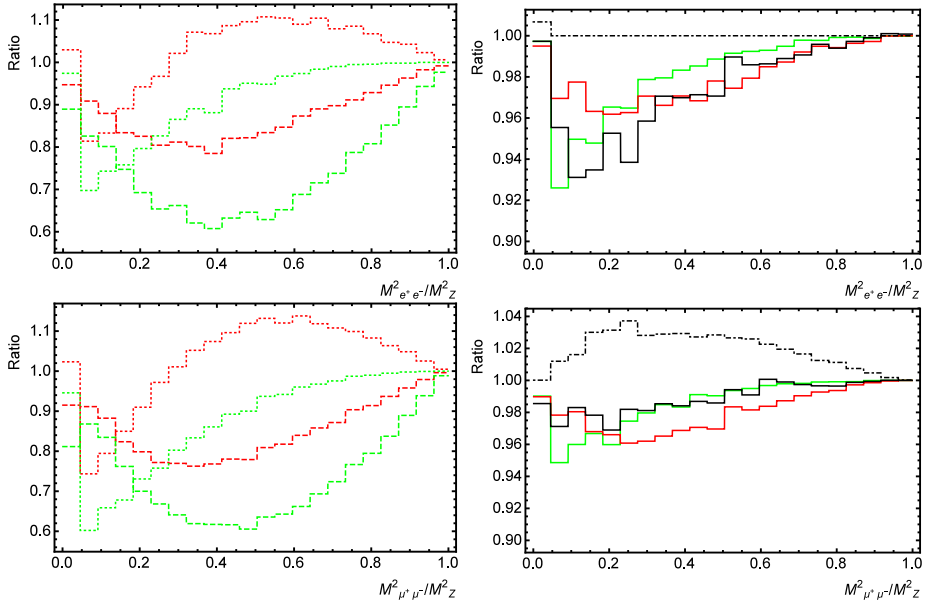


Fig. 4. Ratios of PHOTOS generated spectra in the channel $Z \rightarrow \mu^+\mu^-e^+e^-$ to the ones that are generated by PHOTOS with matrix element (4). Top and bottom left: Grey (green) dashed line represents data corresponding to the absence of the tensor $H_1^{\mu,\nu}$ in matrix element (4); grey (green) dotted line — tensor $H_2^{\mu,\nu}$, black (red) dashed line — tensor $H_3^{\mu,\nu}$, black (red) dotted line — tensor $H_4^{\mu,\nu}$. Top and bottom right: Black dash-dotted line — absence of tensor $H_5^{\mu,\nu}$, light grey (green) solid line — tensor $H_6^{\mu,\nu}$, dark grey (red) solid line — tensor $H_7^{\mu,\nu}$, black solid — tensor $H_8^{\mu,\nu}$.

4. Summary

Exact matrix element (4) of $2f \rightarrow Z/\gamma^* \rightarrow 4f$ process is calculated and presented as the Lorentz contraction of initial-state tensor and the sum of final-state tensors (5)–(12). Tensors, corresponding to the final state of Eq. (4), are exact. If photon is an intermediate particle, the final-state tensors of Eq. (4) can be used together with any possible initial state. If Z boson is an intermediate particle, final-state tensors of Eq. (4) cover the case of unpolarized Z -boson production and decay. Matrix element (4) is a good basis for calculation of the matrix element corresponding to polarized Z -boson production and decay.

Agreement between PHOTOS and KORALW for $2f \rightarrow Z/\gamma^* \rightarrow 4f$ process is reached. Numerical effect of the each of tensors (5)–(12) on extra pair generation is analyzed. Basing on that effect, tensors (9)–(12) can be neglected in matrix element (4). This approximation may lead to factorization of matrix element (4).

REFERENCES

- [1] ATLAS Collaboration (M. Aaboud *et al.*), *Eur. Phys. J. C* **78**, 110 (2018); *Erratum ibid.* **78**, 898 (2018).
- [2] C.M. Carloni Calame *et al.*, *Phys. Rev. D* **96**, 093005 (2017), [arXiv:1612.02841 \[hep-ph\]](https://arxiv.org/abs/1612.02841).
- [3] E. Barberio, B. van Eijk, Z. Wař, *Comput. Phys. Commun.* **66**, 115 (1991).
- [4] E. Barberio, Z. Wař, *Comput. Phys. Commun.* **79**, 291 (1994).
- [5] P. Golonka, Z. Was, *Eur. Phys. J. C* **45**, 97 (2006), [arXiv:hep-ph/0506026](https://arxiv.org/abs/hep-ph/0506026).
- [6] G. Nanava, Z. Wař, *Eur. Phys. J. C* **51**, 569 (2007), [arXiv:hep-ph/0607019](https://arxiv.org/abs/hep-ph/0607019).
- [7] P. Golonka, Z. Wař, *Eur. Phys. J. C* **50**, 53 (2007), [arXiv:hep-ph/0604232](https://arxiv.org/abs/hep-ph/0604232).
- [8] G. Nanava, Q. Xu, Z. Wař, *Eur. Phys. J. C* **70**, 673 (2010), [arXiv:0906.4052 \[hep-ph\]](https://arxiv.org/abs/0906.4052).
- [9] N. Davidson, T. Przedzinski, Z. Was, *Comput. Phys. Commun.* **199**, 86 (2016), [arXiv:1011.0937 \[hep-ph\]](https://arxiv.org/abs/1011.0937).
- [10] S. Jadach, M. Skrzypek, B.F.L. Ward, *Phys. Rev. D* **49**, 1178 (1994).
- [11] S. Jadach *et al.*, *Comput. Phys. Commun.* **119**, 272 (1999), [arXiv:hep-ph/9906277](https://arxiv.org/abs/hep-ph/9906277).
- [12] S. Antropov, A. Arbuzov, R. Sadykov, Z. Was, *Acta Phys. Pol. B* **48**, 1469 (2017), [arXiv:1706.05571 \[hep-ph\]](https://arxiv.org/abs/1706.05571).
- [13] «Comparison of extra lepton pair emission by PHOTOS and by KORALW», <http://annapurna.ifj.edu.pl/%7Ewasm/mumumumu.pdf>
<http://annapurna.ifj.edu.pl/%7Ewasm/eemumu.pdf>
- [14] T. Sjöstrand, S. Mrenna, P.Z. Skands, *Comput. Phys. Commun.* **178**, 852 (2008), [arXiv:0710.3820 \[hep-ph\]](https://arxiv.org/abs/0710.3820).